Appl. Phys. B 71, 585–591 (2000) / Digital Object Identifier (DOI) 10.1007/s003400000377

Applied Physics B
Lasers
and Optics

Measurement of gas jet flow velocities using laser-induced electrostrictive gratings

D.N. Kozlov[1], **B. Hemmerling**[2], **A. Stampanoni-Panariello**[2]

[1] General Physics Institute, Vavilov str. 38, 117942 Moscow, Russia
(Fax: +7-095/135-0297, E-mail: dnk@kapella.gpi.ru)
[2] Paul Scherrer Institut, CH-5232 Villigen PSI, Switzerland
(Fax: +41-056/310-2199, E-mail: Bernd.Hemmerling@psi.ch; Anna.Stampanoni@psi.ch)

Received: 8 Febuary 2000/Revised version: 2 May 2000/Published online: 2 August 2000 –

Abstract. We used time-resolved light scattering of cw probe laser radiation from laser-induced electrostrictive gratings for the determination of flow velocities in air at room temperature. Some possibilities of the technique have been experimentally demonstrated with submerged planar air jets in atmosphere, both for accumulated and single-shot measurements. The range of investigated flow velocities was 5–200 m/s. The method of data treatment and of the estimate of the experimental parameters is described.

PACS: 42.62.-b; 47.62.+q; 43.58.+z

To characterise a reacting gas flow, as represented for example by a flame, one has to perform local measurements of temperature, density, and velocity. Various four-wave mixing techniques, in particular coherent anti-Stokes Raman scattering (CARS) [1], have been used for the non-intrusive determination of temperature and density. Modern systems for flow velocity measurements have attained a high level of technological development. Laser Doppler anemometry (LDA) [2] and particle imaging velocimetry (PIV) [3] became commercially available during recent years. However, these methods rely on seeding of the flow with particles, which narrows the field of their applicability. Flow velocity measurements without seeding have been accomplished employing Doppler shift of atomic or molecular absorption or Raman frequencies detected by either linear [4] or non-linear [5–7] optical methods. Rayleigh scattering has also been regarded as a method to perform flow velocity measurements in pure gases [8]. The flow tagging technique [9] needs no seeding and is based on marking the flow components with one laser and monitoring the temporal evolution of the marked species in space with another laser.

Recently, it was proposed to determine jet flow velocities by employing resonantly excited laser-induced thermal gratings in a moving gas and by accomplishing the interferometric measurements of the Doppler frequency shift of the scattered probe laser pulse [10]. Alternatively, if a laser-induced grating is formed by a pulsed laser and a cw laser is used to read it out, the temporal evolution of the grating can be followed. In the present paper we report, for the first time, on the experimental demonstration of the possibility to use the analysis of the temporal evolution of non-resonantly excited laser-induced electrostrictive gratings for the determination of flow velocities.

1 Theoretical considerations

1.1 Laser-induced gratings

Laser-induced gratings are spatial modulations of the complex refractive index of a medium produced by the field of the interference pattern, which is formed by two equally polarized pump laser beams [11–14]. The beams have the wave vectors $\boldsymbol{k}_1$ and $\boldsymbol{k}_2$ and intersect at an angle θ_P (see Fig. 1a). Laser-induced electrostrictive gratings (LIEGs) are generated by pump laser beams of arbitrary wavelength λ_P. The electric field of the interference pattern polarizes the medium, and the spatial inhomogeneity of the field exerts a force acting inside the medium. As a result, ultrasound waves are generated, with their wavelength defined by the fringe spacing of the interference pattern

$$\Lambda = \lambda_\mathrm{P}/2\sin(\theta_\mathrm{P}/2) = 2\pi/|\boldsymbol{q}|, \quad \boldsymbol{q} = \boldsymbol{k}_1 - \boldsymbol{k}_2. \tag{1}$$

These ultrasound waves are spatially overlapping and propagate in opposite directions along the x axis with the wave vectors $\boldsymbol{q}$ and $-\boldsymbol{q}$, normal to the planes of the fringes (see Fig. 1a), thus forming a standing wave and thereby a spatially periodic density variation that oscillates in time. The effective length of the grating L along the y axis (the length of the volume excited by the pump beams) can be estimated as

$$L \cong 2(w_0/\sqrt{2})/\sin(\theta_\mathrm{P}/2) = \sqrt{2}\Lambda(2w_0/\lambda_\mathrm{P}) \gg \Lambda, \tag{2}$$

where $2w_0$ is the diameter of the pump beams in the crossing area. Such gratings can be efficiently read-out by radiation from another laser with arbitrary wavelength λ_R using Bragg diffraction (coherent scattering). In this case the angle θ_R between the wave vector $\boldsymbol{k}_\mathrm{R}$ of the read-out beam and the planes

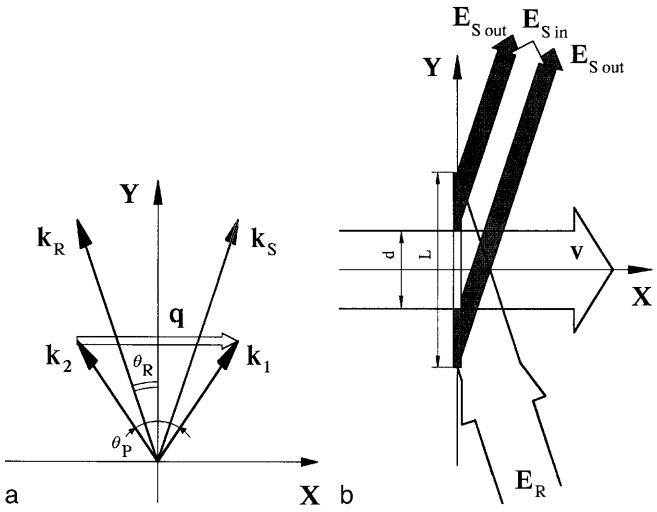

Fig. 1a,b. The scheme of the interaction of the laser beams in the course of excitation and probing of laser-induced gratings: **a** a grating in a homogeneous medium; **b** scattering from a grating simultaneously excited both inside and outside the spatially limited flow; the part of the probe volume located outside the flow, in the gas at rest, and the corresponding contributions to the scattered radiation, are shown with hatching

of the fringes should be given by the relation:

$$\sin\theta_R = (\lambda_R/\lambda_P)\sin(\theta_P/2). \tag{3}$$

The requirement for Bragg diffraction $\lambda_R L/\Lambda^2 > 1$, expressed in our case as $\sqrt{2}(\lambda_R/\lambda_P)(2w_0/\Lambda) > 1$, can be easily satisfied by the appropriate choice of $\lambda_P, \lambda_R, 2w_0$ and the geometry of the experiment.

If there is no absorption at the wavelength λ_R of the read-out beam the scattering efficiency η of a laser-induced grating is [11]:

$$\eta = \frac{P_S}{P_R} = \left[\frac{\pi L}{\lambda_R}\delta n\right]^2 \approx \left[\frac{\pi L}{\lambda_R}\left(\frac{\partial n}{\partial \varrho}\right)_T \delta\varrho\right]^2. \tag{4}$$

Here, P_S and P_R are the powers of the scattered and of the read-out laser beams, whereas δn and δp are the variations of the refractive index and the equilibrium gas density across a fringe of the grating. Equation 4 takes into account that the dependence of the refractive index on temperature is usually small in a gas and can be neglected as compared to the change of the refractive index caused by the variation of gas density $\delta\varrho$.

The density variations affected by electrostriction can be quantitatively described using the linearized hydrodynamic equations [13, 14]. The solution of these equations, which is obtained under the conditions of weak acoustic damping, is a superposition of a standing ultrasound wave, created by electrostrictive adiabatic compression of the medium, and a stationary density modulation, due to the local temperature variation resulting from the adiabatic compression. Compared to the density variation caused by the standing ultrasound wave, the stationary density modulation is small and can be neglected. For the excitation by an infinitely short laser pulse at the initial moment $t = 0$ this solution can be expressed at $t > 0$ as

$$\delta\varrho \cong A\{\sin\Omega t\exp(-t/\tau_a)\}\cos(qx), \tag{5}$$

where the frequency of the standing ultrasound wave $\Omega = 2\pi v_s/\Lambda$ is determined by the adiabatic sound velocity v_s, τ_a is the damping constant of the ultrasound wave, and x is the coordinate along the direction of $\boldsymbol{q}$. The scale factor A in (5) is determined as

$$A = \frac{4\pi}{\Lambda v_s c}\gamma_e\left[(W_1W_2)^{1/2}\Big/S\right]. \tag{6}$$

Here, $\gamma_e = \varrho_0(\partial\varepsilon/\partial\varrho)$ denotes the electrostrictive constant, with ϱ_0 and ε being the equilibrium (i.e. spatially homogeneous) mass density and the dielectric constant, respectively, c is the speed of light, $W_{1,2}$ are the pump pulse energies, and S is the cross section of the pump beams. Hence, in accordance with (4) and (5), the temporal evolution of the power of the beam, diffracted on the standing acoustic wave, shows a regular high-frequency oscillation with a period $\pi/\Omega = T_a/2$, where $T_a = \Lambda/v_s$ is the acoustic wave period. In an ideal gas, the adiabatic sound velocity is independent on pressure, and is given by (see for example [15])

$$v_s = \sqrt{\gamma\frac{R}{M}T}, \tag{7}$$

where T denotes the temperature, $\gamma = c_p/c_V$ the ratio of the specific heat at constant pressure and volume, M the molar mass, and R the universal gas constant. In a real gas there is, however, a weak dependence of v_s on pressure.

The amplitude of an ultrasound wave in a gas is damped due to viscosity and heat conduction:

$$\tau_a = 2\left(\frac{\Lambda}{2\pi}\right)^2\left\{\frac{1}{\varrho_0}\left[\frac{4}{3}\mu + (\gamma-1)\frac{\kappa}{c_p}\right]\right\}^{-1}, \tag{8}$$

where μ is the dynamic viscosity, and κ is the thermal conductivity. The time constant τ_a scales as Λ^2 and is proportional to the gas density ϱ_0, so that the conditions of weak acoustic damping $T_a/2\pi \ll \tau_a$ are fulfilled the better the higher the density is. However, usually in the experiments the focused beams are employed, so that the oscillation of η usually decays faster than can be expected based on the estimated value of τ_a. In this case the decay time constant is primarily determined by the rate of the relative displacement of the two initially overlapped and counter-propagating ultrasound wave packets, which form the standing wave. For beams with a Gaussian profile of the transverse intensity distribution the decay of the oscillation of the LIEG scattering efficiency due to this displacement can be characterised by $\tau_{tr} = w_0/\sqrt{2}v_s$ (acoustic transit time). To describe the effect quantitatively with reasonable accuracy, the damping factor $\exp(-t/\tau_a)$ in (5) should be replaced by $\exp(-t/\tau_a - t^2/\tau_{tr}^2)$. If $\tau_{tr} \ll \tau_a$ the influence of τ_a is negligible.

The spatial resolution of the LIEG technique along the y axis (the bisectrix of angle θ_P) is determined by the effective length of the grating L. In accordance with (2), $L \sim \Lambda w_0$, and the spatial resolution can be improved, if required (i.e. L can be decreased), at the expense of a reduction of Λ, by enhancement of the intersection angle θ_P, and/or a reduction of w_0, by tighter focusing of the pump beams. Employing (2) and (4)–(6) it can be easily shown that for the scattering efficiency η of a LIEG the relation is valid: $\eta \sim (L\delta\varrho)^2 \sim w_0^{-2}$. Thus, with the improvement of the spatial resolution the peak

power of the scattered radiation remains constant if Λ is reduced, or is growing if w_0 is reduced. In this case it should be noted that with the reduction of parameters Λ and w_0 the decay time constants $\tau_a \sim \Lambda^2$ and $\tau_{tr} \sim w_0$ are also decreasing, The minimum of these two values determines the life-time of a LIEG and the number of the observed oscillation peaks of the scattering efficiency η, respectively. Thus, the decrease of L, if needed, should be started from the reduction of that parameter, Λ or w_0, which corresponds to the maximum decay time constant at a given experimental configuration.

1.2 Method of flow velocity measurement

In the case when a LIEG is excited inside a flow, the central frequency of the scattered light experiences a Doppler shift proportional to the projection of the flow velocity to the vector $\boldsymbol{q}$. Besides interferometric measurements, this shift can be determined by applying the usual heterodyne light detection scheme, through mixing of the frequency-shifted scattered radiation with the reference one, at the un-shifted frequency of the read-out beam, and measuring a beating frequency in a signal from a photodetector. At the measurements in spatially-limited flows (jets) the radiation scattered by a LIEG, which is simultaneously excited in the ambient quiscent gas if the length of the excited volume exceeds the width of the jet, can be employed as a reference radiation, with the central frequency equal to that of the read-out beam.

Such an approach has been realized in our experiments, where all the measurements were carried out in submerged planar air flows produced by a slot nozzle at room temperature. The plane of the nozzle was aligned to be parallel to the x, y plane defined by the wave vectors $\boldsymbol{k}_1$ and $\boldsymbol{k}_2$ of the two pump beams, with the wide side of the slot directed along the y axis. The effective length of the grating exceeded the width of the slot, so that the LIEG was located partly inside and partly outside the jet flow.

In the plane-waves approximation the field of the read-out radiation is

$$E_R(\boldsymbol{r}, t) = E_R(t) \exp(-i\omega_R t + i\boldsymbol{k}_R \boldsymbol{r}) + \text{c.c.}, \tag{9}$$

where $E_R(t)$ is the complex wave amplitude, and ω_R is the angular frequency. Correspondingly, the field of the radiation, which is scattered by the standing ultrasound wave in the direction $\boldsymbol{k}_S = \boldsymbol{k}_R + \boldsymbol{q}$, is given by

$$E_S(\boldsymbol{r}, t) = E_S(t) \exp(-i\omega_R t + i\boldsymbol{k}_S \boldsymbol{r}) + \text{c.c.}. \tag{10}$$

The complex amplitude $E_S(t)$ inside the medium which moves with the velocity $\boldsymbol{v}$ along the x axis can be expressed, in accordance with (4) and (5) and taking into account the Doppler effect, as

$$E_S(t) \propto L\left(n\varrho_0/v_s\right)(\partial n/\partial\varrho)^2 \delta\varrho \exp(i\boldsymbol{q}\boldsymbol{v}t) \times \sin\Omega t \exp(-t/\tau_a). \tag{11}$$

Here the relation $\gamma_e = \varrho_0(\partial\varepsilon/\partial\varrho) \approx 2n\varrho_0(\partial n/\partial\varrho)$ was used. When a part of the excitation and probe volume is inside the flow and the other part of it is located outside, in quiescent gas, as it was in our experiments, the coherently scattered radiation field outside the probe volume is a sum of contributions from these two areas: $E_S(t) = E_{S\,in}(t) + E_{S\,out}(t)$ (see Fig. 1b). For the case of a quasi-rectangular velocity distribution along the length of the probe volume, i.e. along the y axis, the amplitudes of the two contributions can be written as

$$E_{S\,in}(t) = B \exp(i(v/v_{s0})\Omega_0 t) \sin\Omega t \exp(-t/\tau_a), \tag{12}$$

and

$$E_{S\,out}(t) = C \sin\Omega_0 t \exp(-t/\tau_{a0}), \tag{13}$$

where the coefficients B and C are determined, in accordance with (11), by the properties of the medium, and by the interaction lengths inside the scattering volumes. Subscript 0 refers to the quiescent gas. The sound velocity and hence the frequency of the acoustic wave inside the flow is defined by the local temperature.

One obtains for the temporal evolution of the scattered power, which is determined by the interference of the contributions from inside and outside the flow,

$$\begin{aligned} P_S(t) \propto E_S E_S^* \propto{}& B^2 \sin^2\Omega t \exp(-2t/\tau_a) \\ &+ C^2 \sin^2\Omega_0 t \exp(-2t/\tau_{a0}) \\ &+ 2BC\cos((v/v_{s0})\Omega_0 t) \\ &\times \sin\Omega t \sin\Omega_0 t \exp(-t/\tau_a - t/\tau_{a0}). \end{aligned} \tag{14}$$

The Doppler shift results in an amplitude modulation of the usual, high-frequency oscillating temporal shape of a LIEG signal, with the low modulation frequency $\Omega_m = (v/v_{s0})\Omega_0$, which is proportional to the jet velocity. If the jet is constituted by the same gas and at the same temperature as the ambient quiescent medium, then $\Omega \approx \Omega_0$, $\tau_a \approx \tau_{a0}$, and (14) reduces to

$$P_S(t) \propto (B^2 + C^2)\{1 + m\cos(\Omega_m t)\} \sin^2\Omega_0 t \exp(-2t/\tau_{a0}), \tag{15}$$

where the modulation coefficient $m = 2BC/(B^2 + C^2)$ is determined by the ratio of the amplitudes of the light scattered from inside and outside the flow. For no flow conditions, i.e. $v = 0$, (15) describes a LIEG of length L, with the scattered power proportional to $(B + C)^2$. For the jet of the same gas and temperature as the ambient medium the modulation coefficient m in (15) reaches its maximum at $L = 2d$, where d is the width of the jet. This value of L is related as described above, via Λ and w_0, to the minimum decay time constant that determines the number N of the observable peaks of the scattering efficiency η and thus defines a minimum measurable flow velocity as $v_{min} \sim v_{s0}/N$. To apply (15) to the case of spatially limited, focused beams the damping factor $\exp(-t/\tau_a)$ has to be replaced, as pointed above, by $\exp(-t/\tau_a - t^2/\tau_{tr}^2)$.

2 Experimental arrangement

The experimental set-up for generation and detection of LIEGs is similar to that one described in [13, 14], and only the most salient features will be repeated here. Two pump beams of parallel, linear polarization, provided by a pulsed Nd:YAG laser at wavelength $\lambda_P = 1064$ nm (10 Hz, 20 mJ, $\Delta v \approx 1.1\ \text{cm}^{-1}$, $\tau_P \approx 5$ ns), are focused by the same telescope

($f = 2500$ mm) and intersect in the measurement region at an angle $\theta_P \approx 1.6°$. The generated laser-induced grating has a fringe spacing $\Lambda \approx 37\,\mu$m. A cw Ar^+-ion laser ($\lambda_R = 515$ nm, 1 W) furnishes the read-out beam. It is focused by a lens ($f = 1000$ mm) and is aligned to enter the interaction volume opposite to the direction of the pump beams at the angle θ_R, that satisfies the Bragg condition given by (3). The coherent radiation scattered by the LIEG is collimated and directed over a distance of about 5 m onto the aperture of a photomultiplier tube. The time-resolved acquisition of the signal is performed by a digital oscilloscope with a full bandwidth of 500 MHz and a 1 GHz sampling rate.

A slot nozzle to produce submerged planar air flows at room temperature $T = 293$ K was $h = 1.5$ mm in height and $d = 18$ mm in width. We manufactured the nozzle by squeezing one end of a copper tube, so that a channel with a quasi-rectangular cross section and a length of about 20 mm was formed. The probe volume was moved as close as possible to the nozzle exit, to a distance of about 1 mm from it. We estimated the effective length of the grating to be $L \approx 70$ mm.

3 Measurements and results

The temporal evolution of the signal, which is obtained from a grating formed in ambient air at the exit of the nozzle without any flow (Fig. 2a), shows a regular high-frequency oscillation with a period $T_a/2 = 54.4$ ns. This oscillation is due to the standing ultrasound wave in the probe volume and decays by acoustic damping and as a result of the finite size of the pump beams. The signal, displayed in Fig. 2a, is averaged over 100 laser shots. Its temporal evolution is well described by (15). We obtained the fringe spacing of the grating $\Lambda = 37.3\,\mu$m from the measured acoustic wave period T_a by using the literature value of the sound velocity in air $v_{s0} = 343.4$ m/s at $T = 293$ K [16]. Transport parameters and heat capacities taken from [16] allow for an estimate of the acoustic damping constant $\tau_a = 2.53\,\mu$s by using (5). This value of τ_a was fixed in the fitting procedure, whereas the acoustic transit time τ_{tr}, regarded as a variable parameter, was determined to be $\tau_{tr} = 1.48\,\mu$s, in accordance with the estimated diameter of the pump beams in the crossing region.

An air flowing through the nozzle leads to the occurrence of a superimposed low-frequency modulation of the signal due to heterodyne mixing of light with Doppler-shifted frequency – from inside the flow, and frequency un-shifted light – from outside the flow (see Fig. 2b). An enhancement of the flow velocity results in a shorter period of this modulation (Fig. 2c). For the wide range of flow velocities employed in our experiments (5–200 m/s) the temporal behaviour of the signal is reasonably well described by (15), with an average value of modulation coefficient $\langle m \rangle = 0.7$. This coefficient was determined from a number of values independently deduced from fits of the temporal evolution of the signal for different flow rates. From the width of the nozzle $d = 18$ mm and an estimated length of the interaction volume $L = 70$ mm one can deduce the modulation coefficient $m = 0.6$. This value is in reasonable agreement with the experiment, as far as a small natural divergence of the jet along the flow axis would result in an enhancement of the jet width and therefore in an increase of the modulation coefficient. Thus, $m = 0.7$ would correspond to the jet width $d = 21$ mm.

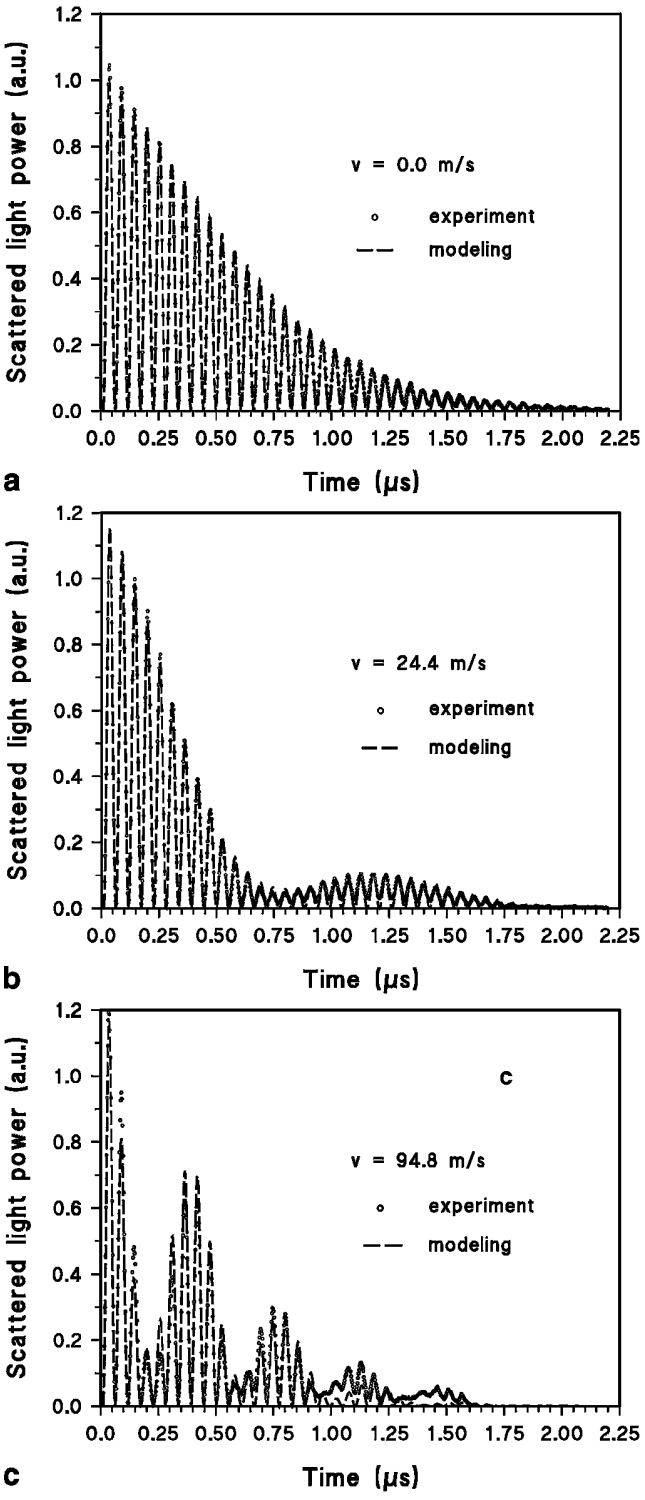

Fig. 2a–c. The temporal evolution of the signals obtained from the LIEGs excited near the edge of a slot nozzle (each of the signals is averaged over 100 laser pulses); *dashed curves* show the best-fit signal profile calculated using (15): **a** in the absence of the flow; **b** in a submerged air jet with $v_Q = 25.2$ m/s; **c** in a submerged air jet with $v_Q = 94.4$ m/s

We verified the proportionality between the frequency Ω_m of the overlaying modulation of the LIEG signal and the air flow rate in the range 10–200 l/min. Figure 3 de-

picts a comparison between the flow velocities v, calculated as $v = v_{s0}(\Omega_m/\Omega_0)$ from the values given by fitting the experimental data, and the average flow velocities v_Q, estimated as $v_Q = Q/S_N$ from flow rates Q and the nozzle cross section S_N. The correlation coefficient of v and v_Q values is 0.9997. However, the proportionality coefficient v/v_Q varies in the range of 1.00–1.15 for independent adjustments of the probe volume position inside the flow. This fact can probably be ascribed to the inhomogeneity of the velocity distribution across the height of the jet (along the z axis) and a small displacement ($x/h \approx 1$) of the probe volume from the nozzle exit. The lower limit of velocities (in fact, frequencies Ω_m) that could be reliably measured is determined by the decay time of a LIEG, which in our case is defined primarily by the acoustic transit time τ_{tr}.

The acoustic wave period T_a was determined at different flow rates as independent fitting parameter of the model and is plotted in Fig. 4 as a function of the average flow velocity v_Q (note that $v_Q \approx v$). Its variation, though relatively small, shows a characteristic quadratic dependence. This is represented by the dashed line in Fig. 4. Apparently, the measured quadratic dependence $T_a \approx T_{a0}(1 + 0.07(v_Q/v_{s0})^2)$ at $(v_Q/v_{s0})^2 \ll 1$ may reflect the slight decrease of the local temperature and hence of the sound velocity $v_s \approx T_a^{-1}$ in the expanding gas flow, that is described by the relation [15]

$$v_s = v_{s0}\sqrt{1 - \frac{(\gamma-1)}{2}\left(v/v_{s0}\right)^2} \approx v_{s0}\left(1 - \frac{(\gamma-1)}{4}\left(v/v_{s0}\right)^2\right), \quad (16)$$

where $(\gamma - 1)/4 = 0.1$ in the case of air. Note that in fact the values of parameter T_a obtained as a result of fitting the signal temporal shapes with (15), that was reduced from the more general (14), are averaged over the width of the jet and besides are somehow intermediate between those for the quiescent gas and the corresponding velocity-dependent characteristic of the gas flow.

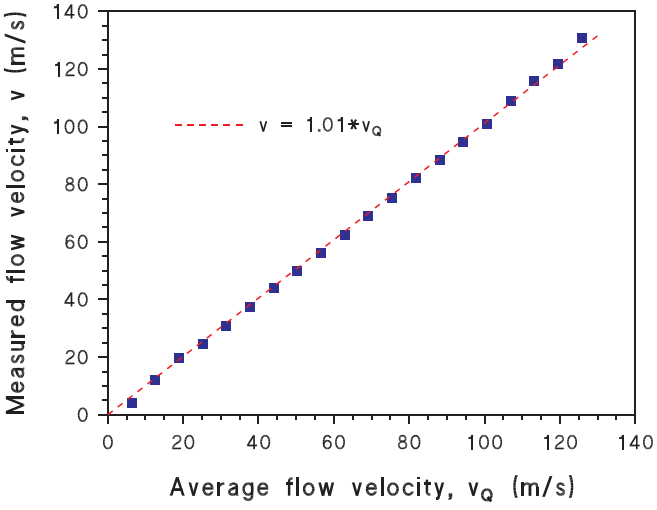

Fig. 3. The correlation between the values of the measured local flow velocity v, at a fixed location of the probe volume as related to the nozzle edge, and average flow velocity v_Q, determined from the gas flow rate and the nozzle cross section. The dashed line shows the linear approximation of the dependence

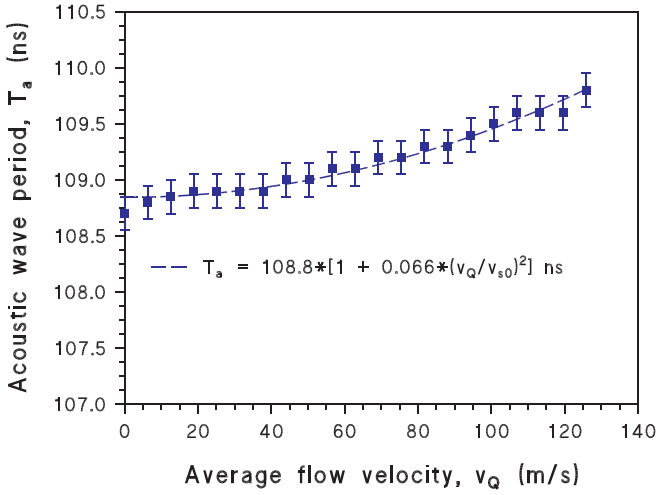

Fig. 4. The dependence of the acoustic wave period T_a on the average flow velocity v_Q. The corresponding approximating function is shown with the *dashed line*

We demonstrate that the LIEG technique allows sound and flow velocities to be measured by a single laser shot (~ 5 ns). Comparing the values derived in a stationary flow from a signal averaged over 100 laser pulses (Fig. 5a) with those from single-shot signals, characterised by significant pulse-to-pulse amplitude noise (see Fig. 5b), one observes a good reproducibility of the sound and flow velocity determination. As a confirmation, Fig. 6 presents the normalized histograms of periods T_a and velocities v obtained from 100 single-shot LIEG signals, that were registered at the same stationary flow conditions ($v_Q = 31.5$ m/s). Both distributions can be reasonably fitted to a Gaussian probability density function, with the standard deviation equal to 0.20 ns (0.2%) for the acoustic wave period T_a and to 1.8 m/s (5%) for the flow velocity v. The slight asymmetry of the velocity distribution at the side of lower values probably corresponds to the observed gradual 4% decrease of the flow rate during the period of data recording.

The high spatial resolution of the LIEG technique in z direction (about 0.2 mm) is demonstrated, for instance, by measurements of the jet velocity profile across the nozzle (Fig. 7). The measurements have been performed with a step of 0.1 mm at a distance $x = 1$ mm ($x/h \approx 0.7$) from the nozzle exit. The velocity distribution obtained is almost flat near the flow axis and steeply varies in the regions of geometrical boundaries of the jet. The value of the modulation coefficient m determined as an independent fitting parameter at different z is practically constant inside the jet ($m \approx 0.73$) and, as expected, sharply decreases near its boundaries (see Fig. 7), in accordance with the fact that the length of the grating located inside the flow becomes shorter. This plagues the determination of smaller velocities in the boundary layers of the jet. Averaging of the velocities over z within the limits $-h/2 \le z \le h/2$ gives $v_Q = 33.3$ m/s, in a fairly good agreement with the experimentally estimated value $v_Q = 32.7$ m/s.

Last but not the least, it should be noted that, together with the determination of the flow velocity, the analysis of the LIEG signal temporal evolution allows for simultaneous gas thermometry in the same probe volume. Temperature can

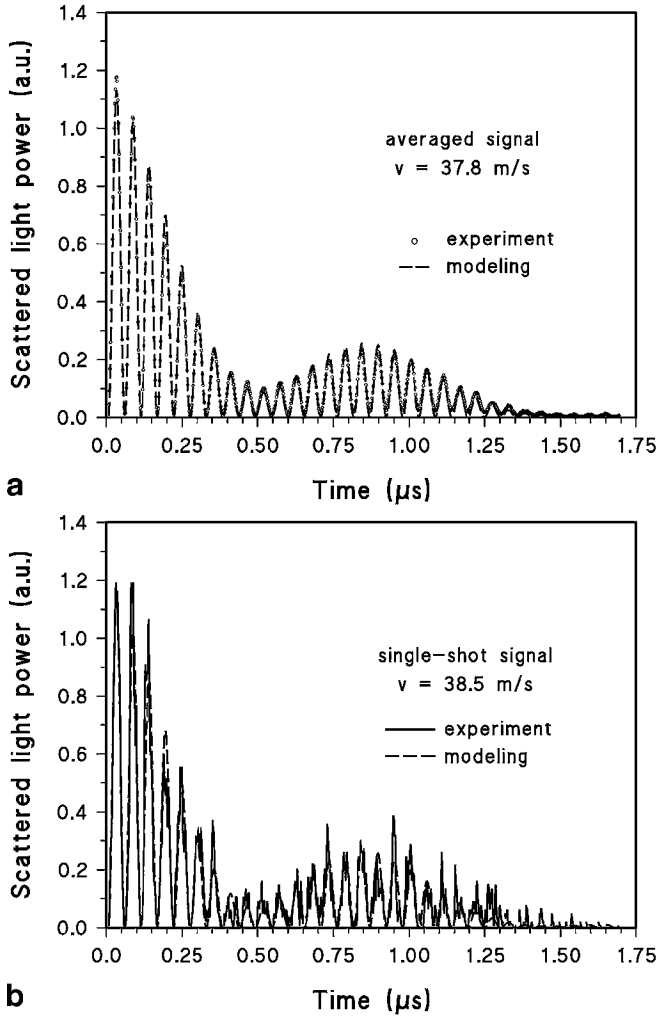

Fig. 5a,b. Comparison of **a** averaged and **b** single-shot LIEG signals, obtained at the same stationary flow conditions ($v_Q = 31.5$ m/s)

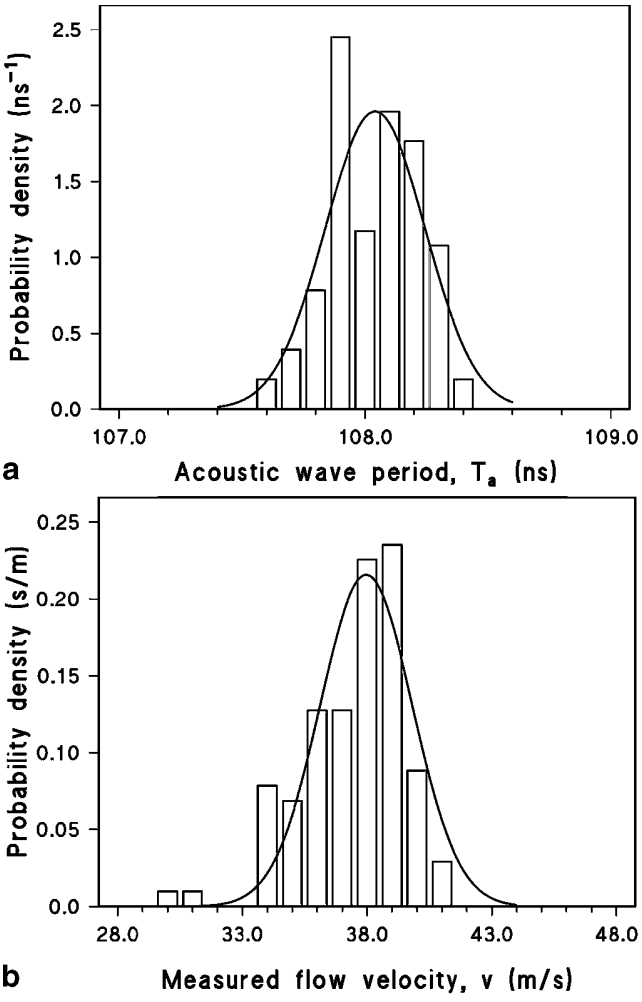

Fig. 6a,b. The normalized histograms of data obtained from 100 single-shot LIEG signals, registered at the stationary flow conditions ($v_Q = 31.5$ m/s): **a** distribution of acoustic wave periods Ta (bin width is 0.1 ns); **b** distribution of flow velocities v (bin width is 1 m/s)

be deduced from the adiabatic sound velocity v_s via (7). This has been demonstrated under conditions of a static heated cell in [17]. The results of LIEG-signals measurements in our experimental configuration, which are presented in Fig. 4 and refer to adiabatically cooled gas flow, also show the promise to obtain information on gas temperature. Experiments with submerged heated jets in room air, aimed at verifying these possibilities of the presented LIEG technique, are now in progress.

4 Conclusion

We demonstrated that time-resolved measurements of power of light scattered from laser-induced electrostrictive gratings can be employed for the determination of jet flow velocities. The principle of the technique consists in local "seeding" of the jet with a laser-induced standing ultrasound wave and heterodyne detection of the radiation scattered by this wave. The method employed provides the feasibility to accomplish not only accumulated, but also single-shot measurements.

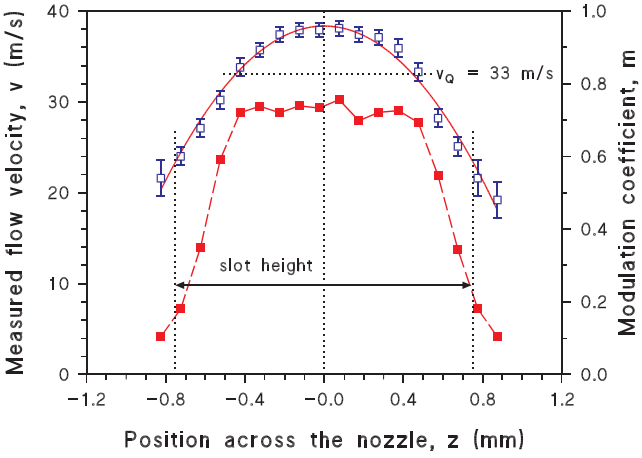

Fig. 7. The measurements of the jet flow velocity (*open squares*) and of the modulation coefficient (*solid squares*) profiles across the height of the nozzle ($v_Q = 32.7$ m/s). The *dashed lines* are the guides for the eye

The possibilities of the technique have been experimentally demonstrated for submerged jet flows in air for a wide range of flow rates. The experiments showed that lower

flow velocities, as compared to those provided by optical interferometric measurements of the Doppler frequency shift of light scattered by a laser-induced grating, can be measured and good precision can be achieved. However, a comparison of data provided by the LIEG technique with the results of already established velocity measuring methods would be of interest to be performed for verification of our approach.

The limitations of the presented experimental technique, such as (a) requirement of the quiescent gas around the flow as a source of the reference wave for heterodyning and (b) low spatial resolution along the length of the probe volume, should be noted. By now, the work has been performed aimed to modify the experimental arrangement in order to be able to employ LIEGs with an effective length shorter than the width of the flow, and the first measurements have been accomplished [18].

The lower limit of measurable flow velocities is determined by the relatively short LIEG decay time, related to acoustic damping constant or acoustic transit time. Possibilities are investigated to use laser-induced thermal gratings for similar measurements, as far as they represent longer-living stationary spatial modulations of the refractive index, so that the determination of smaller flow velocities should become feasible.

Acknowledgements. The financial support of the Swiss Federal Office of Energy (BFE) is gratefully acknowledged. DNK is grateful to BMBF, Germany, for the financial support (grant No.13N7281) and would also like to thank O. Stel'makh for valuable discussions.

References

1. D.A. Greenhalgh: In *Advances in Non-Linear Spectroscopy*, ed. by. R.J.H. Clark, R.E. Hester (Wiley, Chichester, New York, Brisbane, Toronto, Singapore 1988)
2. R.J. Goldstein: *Fluid Mechanics Measurements* (Hemisphere 1983)
3. I. Grant: Proc. of the Inst. of Mech. Engineers C **211**, 55 (1997)
4. A.Y. Chang, M.D. DiRosa, D.F. Davidson, R.K. Hanson: Appl. Opt. **30**, 3011 (1991)
5. E.K. Gustafson, J.D. McDaniel, R.L. Byer: IEEE. J. Quantum Electron. **QE-17**, 2259 (1981)
6. G.C. Herring, S.A. Lee, C.Y. She: Opt. Lett. **8**, 214 (1983)
7. R.B. Williams, P. Ewart, A. Dreizler: Opt. Lett. **19**, 1486 (1994)
8. R.B. Miles, W.R. Lempert: Appl. Phys. B **51**, 1 (1990); J.N. Forkey, N.D. Finkelstein, W.R. Lempert, R.B. Miles: AIAA J. **34**, 442 (1996)
9. R.B. Miles, D. Zhou, B. Zhang, W.R. Lempert: AIAA J. **31**, 447 (1993)
10. D.J.W. Walker, R.B. Williams, P. Ewart: Opt. Lett. **23** 1316 (1998)
11. H.J. Eichler, P. Günter, D.W. Pohl: *Laser-induced Dynamic Gratings* (Springer, Berlin, Heidelberg 1986)
12. D.E. Govoni, J.A. Booze, A. Sinha, F.F. Crim: Chem. Phys. Lett. **216**, 525 (1993)
13. A. Stampanoni-Panariello, B. Hemmerling, W. Hubschmid: Phys. Rev. A **51**, 655 (1995)
14. W. Hubschmid, B. Hemmerling, A. Stampanoni-Panariello: J. Opt. Soc. Am. B **12**, 1850 (1995)
15. L.D. Landau, E.M. Lifshitz: *Course of Theoretical Physics.* V.6. *Fluid Mechanics* (Pergamon Press, Oxford, New York, Beijing, Frankfurt, Sao Paulo, Sydney, Tokio, Toronto 1987)
16. G.W.C. Kaye, T.H. Laby: *Tables of Physical and Chemical Constants* (Longmans Green, New York 1986)
17. A. Stampanoni-Panariello, B. Hemmerling, W. Hubschmid: Appl. Phys. B **67**, 125 (1998)
18. B. Hemmerling, D.N. Kozlov, A. Stampanoni-Panariello: to be published